Multi-LED Transmission Schemes using OTFS Modulation in Visible Light Communication

Sujata Sinha and A. Chockalingam
Department of ECE, Indian Institute of Science, Bangalore 560012

***Abstract*—Orthogonal time frequency space (OTFS) modulation is a recently introduced modulation which has been shown to perform better than OFDM in RF wireless communications. In this paper, we investigate OTFS in multi-LED indoor visible light wireless communications. We propose two multi-LED OTFS schemes, namely, quadrature spatial modulation OTFS (QSM-OTFS) scheme and dual mode index modulation OTFS (DMIM-OTFS) scheme. The proposed schemes use dual-LED complex modulation as the basic building block and offer enhanced rates compared to conventional index modulation schemes. The schemes also have the advantage of not requiring Hermitian symmetry and DC bias operations to obtain real, positive-valued signals suited for intensity modulation of LEDs. We obtain upper bounds on the bit error rate performance of the proposed schemes, which are tight at high signal-to-noise ratios. The proposed OTFS schemes are shown to perform better than their OFDM counterparts known in the literature. In addition, the spatial distribution of the performance gap between OTFS and OFDM across the room is captured using the ratio of the minimum distance of normalized received signal sets of the considered schemes as a metric.**

Keywords: *Visible light communication, OTFS modulation, multi-LED transmission, QSM-OTFS, DMIM-OTFS.*

I. Introduction

Visible light communication (VLC) technology is emerging as an attractive technology for wireless communications in indoor and vehicular environments [1]-[3]. Recently, in radio frequency (RF) based wireless communications, a new modulation scheme called orthogonal time frequency space (OTFS) modulation has attracted lot of research interest [4]. OTFS is a two-dimensional (2D) modulation scheme, where NM information symbols are multiplexed in the delay-Doppler (DD) domain using N delay bins and M Doppler bins. These symbols in the DD domain are mapped to time domain for transmission using 2D transformations. OTFS has been shown to achieve signficantly superior performance compared to OFDM in high-mobility as well as static channel conditions [4]-[8]. This has motivated the investigation of this new modulation in the context of wireless communication using visible light spectrum. It is of interest to see how OTFS performs compared to OFDM in VLC environments. An early investigation in this regard has been reported recently in [9]. The study in [9] has considered OTFS in a single-LED DC-biased optical (DCO) scheme and showed that DCO-OTFS can perform significantly better than DCO-OFDM. This promising result further motivates the need for more OTFS research in VLC systems, which forms the basis for this paper.

This work was supported in part by the J. C. Bose National Fellowship, Department of Science and Technology, Government of India, and the Centre for Networked Intelligence (a Cisco CSR initiative) of the Indian Institute of Science, Bangalore.

We propose two promising multi-LED VLC transmitter architectures employing OTFS. These schemes are inspired by RF index modulation schemes, namely, quadrature spatial modulation (QSM) [10] and dual mode index modulation (DMIM) [11]. We consider these schemes because they offer enhanced rates compared to conventional index modulation schemes. We refer the proposed schemes as QSM-OTFS and DMIM-OTFS schemes. We realize the proposed schemes using dual-LED complex modulation (DCM) block [12], [13] as the basic building block. In both the proposed schemes, the available LEDs are grouped in to multiple DCM blocks. Each DCM block consists of a pair of LEDs, one LED to transmit the magnitude and the other LED to transmit the phase of complex signals that convey information bits. In addition, the choice of the LED pair (among the available pairs) to transmit the complex signals in a given channel use convey additional index bits. Both the proposed architectures avoid the Hermitian symmetry operation (that causes rate loss) and DC-bias often used in conventional approaches to generate positive-valued real signals compatible for intensity modulation of LEDs. The new contributions in this paper can be summarized as follows.

- We obtain analytical upper bounds on the bit error rate (BER) performance of the proposed QSM-OTFS and DMIM-OTFS schemes, which are found to be tight at high signal-to-noise ratios (SNR).
- Our analytical and simulation results show that the proposed QSM-OTFS and DMIM-OTFS schemes achieve better performance compared to their OFDM counterparts in the VLC literature (i.e., QSM-OFDM, DMIM-OFDM).
- Further, using the ratio of the minimum distance of different normalized received signal sets as a metric, we quantify the spatial distribution of the SNR gain in the proposed OTFS schemes compared to their OFDM counterparts.

II. Indoor VLC system model

Consider an indoor MIMO VLC system consisting of N_t transmit LEDs and N_r receive PDs in a room of dimension 5m $\times$ 5m $\times$ 3.5m as shown in Fig. 1. Each LED is either OFF or emits some intensity whose magnitude is based on the complex modulated signal sent in each channel use. The proposed schemes are block transmission schemes that employ multiple channel uses (say, Q channel uses) for transmission. Let $\mathbf{S}$ denote the $N_t \times Q$ transmit matrix, given by

$$\mathbf{S} = \begin{bmatrix} s[1,1] & s[1,2] & \cdots & s[1,Q] \\ s[2,1] & s[2,2] & \cdots & s[2,Q] \\ \vdots & \vdots & \ddots & \vdots \\ s[N_t,1] & s[N_t,2] & \cdots & s[N_t,Q] \end{bmatrix},$$

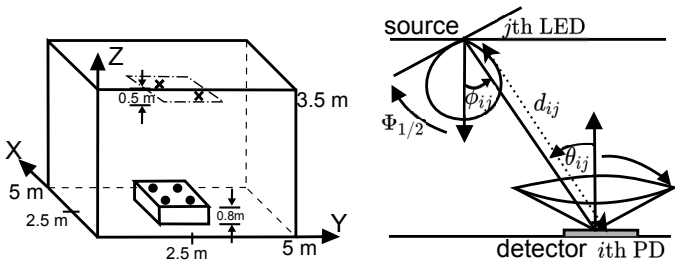

Fig. 1: Indoor VLC system setup. A cross represents an LED and a dot represents a PD.

where $s[j,q]$ denotes the intensity of light transmitted by the jth LED in the qth channel use. We assume that the LEDs have Lambertian radiation pattern. We consider a static channel with line-of-sight (LOS) paths between the LEDs and the PDs. The channel matrix $\mathbf{H}$ is of order $N_r \times N_t$, whose (i,j)th element h_{ij} is the LOS channel gain between the jth LED and ith PD, given by [1]

$$h_{ij} = \frac{n+1}{2\pi}\cos^n\phi_{ij}\cos\theta_{ij}\frac{A}{d_{ij}^2}\,\mathrm{rect}\left(\frac{\theta_{ij}}{FOV}\right), \qquad (1)$$

where n is the mode number of the LED radiation pattern, ϕ_{ij} is the angle of emergence from the jth LED towards the ith PD, A is the area of the PD, d_{ij} is the distance between the jth LED and the ith PD, θ_{ij} is the angle of incidence at the ith PD from the jth LED, FOV is the field-of-view of the PD, and rect(x) = 0, for all $|x| > 1$, where $|\cdot|$ represents the absolute value operator or cardinality of a set. The mode number is given by $n = \frac{-\ln(2)}{\ln\cos\Phi_{\frac{1}{2}}}$, where $\Phi_{\frac{1}{2}}$ is the half power semi-angle of the LED. Assuming perfect channel knowledge and synchronisation at the receiver, the received matrix $\mathbf{Y}$ of order $N_r \times Q$ can be written as

$$\mathbf{Y} = r\mathbf{H}\mathbf{S} + \mathbf{N}, \qquad (2)$$

where r is the responsivity of the PD in Amps/Watt and $\mathbf{N}$ is the $N_r \times Q$ noise matrix. Each element in $\mathbf{N}$ is the sum of thermal noise and ambient shot noise which is modelled as i.i.d. Gaussian with zero mean and variance σ^2. The average SNR is given by $\bar{\gamma} = \frac{r^2}{\sigma^2 N_r}\sum_{i=1}^{N_r}\mathbb{E}[|\mathbf{h}_i\mathbf{S}|^2]$, where $\mathbf{h}_i$ is the ith row of $\mathbf{H}$.

Note 1: The LEDs are placed 0.5 m below the ceiling of the room with d_{tx} as the distance between the LEDs as shown in Fig. 2(a). The placement of the receiver is as shown in Fig 2(b). The coordinate of the receiver location on the receiver plane (which is 0.8 m above the ground) is denoted by (X_R, Y_R). The receiver is assumed to have $N_r = 4$ PDs placed at the corners of a square of side d_{rx} and center (X_R, Y_R). We will vary the location of the receiver in the receiver plane and obtain the spatial distribution of the system performance.

III. Proposed QSM-OTFS and DMIM-OTFS schemes

A. Proposed QSM-OTFS scheme

The proposed QSM-OTFS scheme uses N_t LEDs, where $N_t = 2^i$ and i is an integer ≥ 2. The scheme uses multiple DCM blocks. Each DCM block consists of a pair of LEDs.

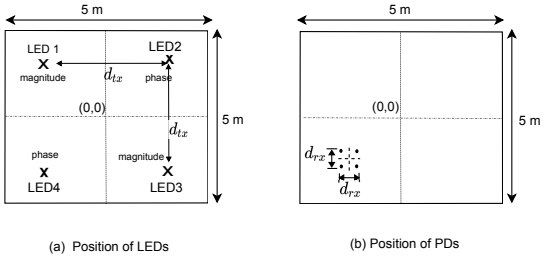

Fig. 2: Placement of the transmitter LEDs and receiver PDs.

The N_t LEDs are divided into $N_q = \frac{N_t}{2}$ DCM blocks. In every NM channel uses, $2\log_2 N_q + NM\log_2|\mathbb{A}|$ bits are conveyed, out of which $2\log_2 N_q$ bits are used for indexing the DCM blocks and $NM\log_2|\mathbb{A}|$ bits are mapped to NM modulation symbols from a modulation alphabet $\mathbb{A}$ (e.g., QAM/PSK), where $|\mathbb{A}|$ is the alphabet size. Figure 3 shows the block diagram of the proposed QSM-OTFS transmitter, where $N_t = 4$ and $N_q = 2$. Two index bits are used to select the transmitting DCM blocks and $NM\log_2|\mathbb{A}|$ bits are mapped to symbols from $|\mathbb{A}|$. The information symbols, denoted by $x[k,l]$, $k = 0,1,\cdots,N-1$, $l = 0,1,\cdots,M-1$, are populated in a matrix $\mathbf{X}_{in}$ of size $N \times M$ in the delay-Doppler (DD) domain. The matrix $\mathbf{X}_{in}$ is converted into a matrix $\mathbf{X}$ in the time-frequency (TF) domain using $N \times M$-point (2D) inverse symplectic finite Fourier transform (ISFFT) operation. The (n,m)th element in $\mathbf{X}$, denoted by $X'[n,m]$, is given by

$$X[n,m] = \frac{1}{MN}\sum_{k=0}^{N-1}\sum_{l=0}^{M-1} x[k,l]e^{j2\pi\left(\frac{nk}{N}-\frac{ml}{M}\right)}, \qquad (3)$$

where $n = 0,1,\cdots,N-1$ and $m = 0,1,\cdots,M-1$. The TF domain complex matrix $\mathbf{X}$ is converted into a time-domain matrix $\bar{\mathbf{S}}$ of size $N \times M$ using M-point Heisenberg transform using M-point IDFT [7], as

$$\bar{\mathbf{S}} = \sqrt{M}\mathbf{F}_M^H\mathbf{X}^T, \qquad (4)$$

where $\mathbf{F}_M^H$ is the M-point IDFT matrix given by $\mathbf{F}_M = \left\{\frac{1}{\sqrt{M}}e^{2\pi j\frac{ml}{M}}\right\}_{m,l=0}^{M-1}$. The (n,m)th element of $\bar{\mathbf{S}}$, denoted by $\bar{S}[n,m]$, is given by $\bar{S}[n,m] = \frac{1}{\sqrt{M}}\sum_{m=0}^{M-1}\mathrm{X}[n,m]e^{j2\pi\frac{ml}{M}}$. The matrix $\bar{\mathbf{S}}$ is then converted into an NM-sized complex vector $\mathbf{s}$ through parallel-to-serial (P/S) conversion. The elements of $\mathbf{s}$ can be written as

$$\mathrm{s}(k) = \mathrm{s}_R(k) + j\mathrm{s}_I(k), \quad k = 0,1,\cdots,NM-1, \qquad (5)$$

where s_R and s_I denote the real and imaginary parts of s.

Let b_1, b_2 denote the two index bits. The (b_1,b_2) combination is used to decide what is transmitted using DCM block 1 (LED1, LED2) and DCM block 2 (LED3, LED4) as follows.

1) If (b_1,b_2) = (0,0), then DCM block 1 transmits s (LED1 transmits $|s|$ and LED2 transmits $\arg(s)$) and DCM block 2 is inactive.
2) If (b_1,b_2) = (0,1), then DCM block 1 transmits s_R (LED1 transmits $|s_R|$ and LED2 transmits $\arg(s_R)$) and DCM block 2 transmits js_I (LED3 transmits $|js_I|$ and LED4 transmits $\arg(js_I)$).

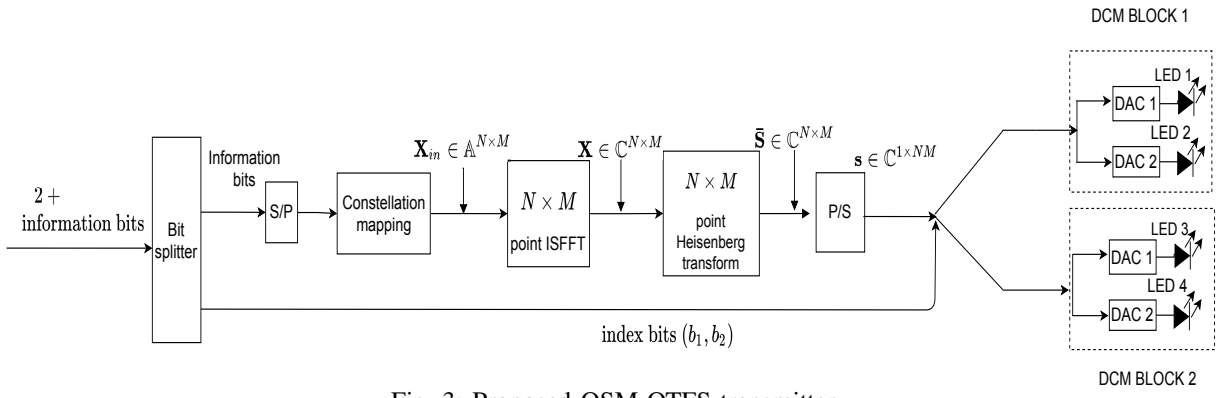

Fig. 3: Proposed QSM-OTFS transmitter.

3) If (b_1, b_2) = (1,0), then DCM block 1 transmits js_I $\big($LED1 transmits $|js_I|$ and LED2 transmits $\arg(js_I)\big)$ and DCM block 2 transmits s_R $\big($LED3 transmits $|s_R|$ and LED4 transmits $\arg(s_R)\big)$.
4) If (b_1, b_2) = (1,1), then DCM block 2 transmits s $\big($LED3 transmits $|s|$ and LED4 transmits $\arg(s)\big)$ and DCM block 1 is inactive.

The transmit intensity values from all four LEDs as described above in NM channel uses constitute a $4 \times NM$ sized QSM-OTFS transmit signal matrix $\mathbf{S}$.

Note 2: The above scheme can be generalized for $N_t = 2^i$, where i is an integer > 2, as follows. $2\log_2 N_q$ index bits are divided into two sets of $\log_2 N_q$ bits. There are N_q indexed DCM blocks. The two sets of bits are used to independently choose the indices of two DCM blocks out of N_q available blocks. If both sets have the same index bits, then both sets select the same DCM block and s is sent from the selected DCM block; else, the DCM block selected by the first set is used to send s_R, i.e., $|s_R|$ and $arg(s_R)$ are transmitted through the magnitude and phase LEDs of the DCM block chosen by the first set of index bits, and, similarly, the DCM block selected by the second set is used to transmit js_I.

It can be seen that $2\log_2 N_q + NM\log_2|\mathbb{A}|$ bits are sent in NM channel uses. Therefore, the achieved rate in QSM-OTFS, in bits per channel use (bpcu), is given by

$$\eta_{\text{qsm-otfs}} = \frac{2\log_2 N_q}{NM} + \log_2|\mathbb{A}| \quad \text{bpcu}. \tag{6}$$

The $N_r \times NM$ received signal matrix $\mathbf{Y}$ corresponding to the transmit signal matrix $\mathbf{S}$ is given by $\mathbf{Y} = r\mathbf{HS} + \mathbf{N}$, and the maximum likelihood (ML) detection rule is given by

$$\hat{\mathbf{S}} = \underset{\mathbf{S}\in\mathbb{S}_{\text{qsm-otfs}}}{\operatorname{argmin}} \|\mathbf{Y} - r\mathbf{HS}\|^2, \tag{7}$$

where $\mathbb{S}_{\text{qsm-otfs}}$ is the set of all QSM-OTFS transmit signal matrices. The information bits are obtained by demapping from the detected matrix $\hat{\mathbf{S}}$ using a lookup table consisting of all transmit signal matrix corresponding to their bit mappings.

B. Proposed DMIM-OTFS scheme

The block diagram of the proposed DMIM-OTFS scheme is shown in Fig. 4 for $N_t = 4$ LEDs and $N_q = \frac{N_t}{2} = 2$ DCM blocks. Here, $\log_2 N_q = 1$ index bit (called *frame index bit*) decides which DCM block among the two will be used to send a given OTFS frame. One LED in the chosen block transmits the magnitude and the other LED transmits the phase of the complex signal. The scheme uses two modulation alphabets, $\mathbb{S}_A$ and $\mathbb{S}_B$, which are chosen to be disjoint (i.e., $\mathbb{S}_A \cap \mathbb{S}_B = \phi$) to distinguish the symbols from the two alphabets. In each OTFS frame, NM symbols are transmitted out of which N_a symbols are from constellation $\mathbb{S}_A$ (group A) and the remaining, $NM - N_a$ symbols are from $\mathbb{S}_B$ (group B). There are $\binom{NM}{N_a}$ possible group patterns for transmitting NM symbols, out of which $2^{\lfloor \log_2 \binom{NM}{N_a} \rfloor}$ patterns are used and $\left\lfloor \log_2 \binom{NM}{N_a} \right\rfloor$ bits (called *group pattern index bits*) are used to index the chosen patterns. $N_a \log_2|\mathbb{S}_A|$ information bits are mapped to symbols from $\mathbb{S}_A$, and $(NM - N_a)\log_2|\mathbb{S}_B|$ information bits mapped to symbols $\mathbb{S}_B$. Therefore, $\log_2 N_q$ frame index bits, $\left\lfloor \log_2 \binom{NM}{N_a} \right\rfloor$ group pattern index bits, and $N_a \log_2|\mathbb{S}_A| + (NM - N_a)\log_2|\mathbb{S}_B|$ modulation bits constitute the total number of bits in a given frame.

As an example, consider the DMIM-OTFS transmitter in Fig. 4 with $N_t = 4$, $N_q = 2$, $M = N = 2$, $N_a = 2$. The number of frame index bits is $\log_2 N_q = 1$. There are $\binom{NM}{N_a} = \binom{4}{2} = 6$ possible group patterns, out of which $2^{\lfloor \log_2 \binom{NM}{N_a} \rfloor} = 4$ patterns are chosen using 2 index bits (b_1, b_2) as follows.

1) If (b_1, b_2) = (0,0), then (A,A,B,B) is the group pattern, i.e., first two symbols are from $\mathbb{S}_A$ while the last two are from $\mathbb{S}_B$.
2) If (b_1, b_2) = (0,1), then (A,B,B,A) is the group pattern, i.e., first and last symbols are from $\mathbb{S}_A$ while the other two are from $\mathbb{S}_B$.
3) If (b_1, b_2) = (1,0), then (B,B,A,A) is the group pattern.
4) If (b_1, b_2) = (1,1), then (B,A,A,B) is the group pattern.

The NM information symbols after mapping to their respective constellation sets are populated in a $N \times M$-sized matrix $\mathbf{X}_{in}$ in the DD domain, which is passed through $N \times M$ point ISFFT operation to obtain the signal matrix $\bar{\mathbf{X}}$ in the TF domain. This TF domain signal matrix is converted into the matrix $\bar{\mathbf{S}}$ in the time domain using Heisenberg transform. The matrix $\bar{\mathbf{S}}$ is converted into a vector $\mathbf{s}$ by P/S conversion. Each element of vector $\mathbf{s}$ is represented in polar form as $s = re^{j\phi}$,

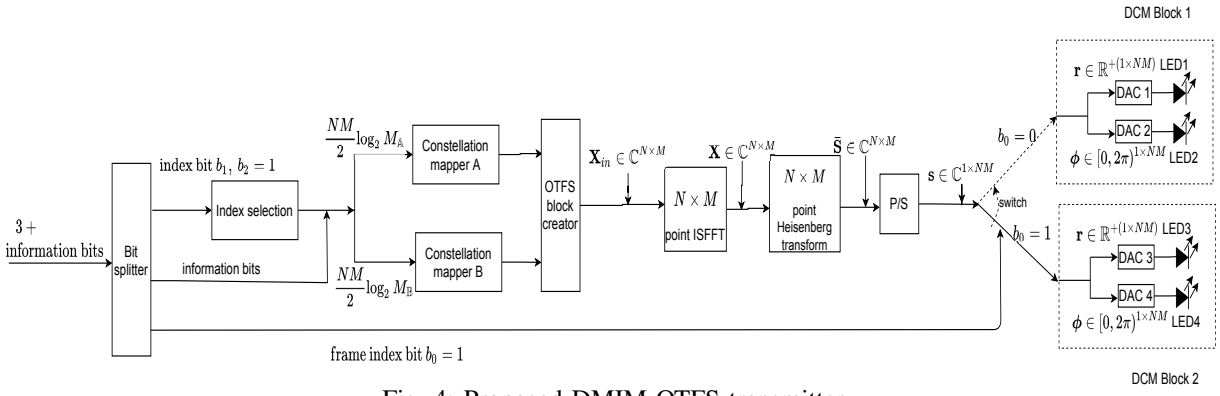

Fig. 4: Proposed DMIM-OTFS transmitter.

where

$$\begin{aligned} r &= |s|, \quad r \in \mathbb{R}^{+} \\ \phi &= \arg(s), \quad \phi \in [0, 2\pi). \end{aligned} \tag{8}$$

Let $\mathbf{r}$ and $\boldsymbol{\phi}$ denote the NM-length magnitude and phase vectors corresponding to the vector $\mathbf{s}$. The transmission of a given OTFS frame is done as follows: 1) if the frame index bit $b_0 = 0$, LED1 and LED2 transmit $\mathbf{r}$ and $\boldsymbol{\phi}$, respectively, and 2) if $b_0 = 1$, LED3 and LED4 transmit $\mathbf{r}$ and $\boldsymbol{\phi}$, respectively. In a given channel use, only one pair of LEDs is on and the other pair remains off, forming a $4 \times NM$ transmission matrix $\mathbf{S}$. This scheme can be generalized for N_q DCM blocks by using $\log_2 N_q$ index bits. As can be seen, in this scheme, $\log_2 N_q + \left\lfloor \log_2 \binom{NM}{N_a} \right\rfloor + N_a \log_2 |\mathbb{S}_A| + (NM - N_a) \log_2 |\mathbb{S}_B|$ information bits are conveyed in NM channel uses. Therefore, the achieved rate in this scheme is given by

$$\eta_{\text{DMIM-OTFS}} = \frac{1}{NM}\Bigg[\log_2 N_q + \left\lfloor \log_2 \binom{NM}{N_a} \right\rfloor + N_a \log_2 |\mathbb{S}_A| + (NM - N_a) \log_2 |\mathbb{S}_B|\Bigg] \text{ bpcu}. \tag{9}$$

ML decision rule is used to detect the DMIM-OTFS matrix from which information bits are recovered through demapping using a lookup table.

IV. Performance analysis

A. Upper bound on BER

Consider the system model in (2) and the corresponding ML decision rule in (7). Normalizing the elements of the noise matrix to variance one, (2) can be written in the form

$$\mathbf{Y} = \frac{r}{\sigma}\mathbf{HS} + \mathbf{N}. \tag{10}$$

The ML decision rule in (7) can be simplified as

$$\hat{\mathbf{S}} = \underset{\mathbf{S}\in\mathbb{S}}{\operatorname{argmin}} \left(\frac{r}{\sigma} \|\mathbf{HS}\|^2 - 2\mathbf{Y}^T\mathbf{HS} \right). \tag{11}$$

Let $\mathbf{S}_1$ and $\mathbf{S}_2$ denote two transmit signal matrices. The pairwise error probability (PEP) of giving a decision in favor of $\mathbf{S}_2$ when $\mathbf{S}_1$ was transmitted can be written as [12]

$$PEP(\mathbf{S}_1 \to \mathbf{S}_2 \mid \mathbf{H}) = Q\left(\frac{r}{2\sigma} \|\mathbf{H}(\mathbf{S}_2 - \mathbf{S}_1)\| \right). \tag{12}$$

An upper bound on the BER can be obtained using union bound as

$$\begin{aligned} p_e &\leq \frac{1}{|\mathbb{S}|MN} \sum_{i=1}^{|\mathbb{S}|} \sum_{j=1, i\neq j}^{|\mathbb{S}|-1} PEP(\mathbf{S}_i \to \mathbf{S}_j \mid \mathbf{H}) \frac{d(\mathbf{S}_i, \mathbf{S}_j)}{\eta} \\ &= \frac{1}{|\mathbb{S}|MN} \sum_{i=1}^{|\mathbb{S}|} \sum_{j=1, i\neq j}^{|\mathbb{S}|-1} Q\left(\frac{r}{2\sigma} \|\mathbf{H}(\mathbf{S}_j - \mathbf{S}_i)\| \right) \frac{d(\mathbf{S}_i, \mathbf{S}_j)}{\eta}, \end{aligned} \tag{13}$$

where $d(\mathbf{S}_i, \mathbf{S}_j)$ is the Hamming distance between bit mappings corresponding to the signal matrices $\mathbf{S}_i$ and $\mathbf{S}_i$, and η is the achieved rate of the system.

B. Normalized minimum distance of received signal sets

Here, we obtain a metric based on the ratio of the normalized minimum distances of the received signal sets of different schemes in order to compare their performance. We use this metric to assess the relative high-SNR performance of different schemes. Suppose $\mathbb{S}_{tx} = \{\mathbf{S}_1, \mathbf{S}_2, \cdots, \mathbf{S}_K\}$ is the set of all possible transmit signal matrices of a particular scheme, where K is the size of the signal set. Let $\mathbb{S}_{rx} = \{\mathbf{HS}_1, \mathbf{HS}_2, \cdots, \mathbf{HS}_K\}$ be the corresponding received signal set in the absence of noise for a given $\mathbf{H}$. The matrices in the set $\mathbb{S}_{rx}$ are normalized by the average received signal power to obtain the normalized received signal set $\tilde{\mathbb{S}}_{rx}$ as $\tilde{\mathbb{S}}_{rx} = \{\tilde{\mathbf{Y}}_1, \tilde{\mathbf{Y}}_2, \cdots, \tilde{\mathbf{Y}}_K\}$, where

$$\tilde{\mathbf{Y}}_i = \frac{\mathbf{HS}_i}{\sqrt{\frac{1}{KN_rMN}\sum_{i=1}^{K} \|\mathbf{HS}_i\|^2}}. \tag{14}$$

The minimum distance of the normalized received signal set $\tilde{\mathbb{S}}_{rx}$ can be obtained as

$$d_{\min,\mathbf{H}} = \min_{\tilde{\mathbf{Y}}_i, \tilde{\mathbf{Y}}_j \in \tilde{\mathbb{S}}_{rx}, i\neq j} \|\tilde{\mathbf{Y}}_i - \tilde{\mathbf{Y}}_j\|_2. \tag{15}$$

Suppose $\mathbb{S}_{tx_1}$ and $\mathbb{S}_{tx_2}$ are the transmit signal sets of two different schemes. For a given $\mathbf{H}$, let $d^{(1)}_{\min,\mathbf{H}}$ and $d^{(2)}_{\min,\mathbf{H}}$ denote the minimum distances of their corresponding normalized received signal sets. Then, at high SNRs, the BER performance of scheme 1 with signal set $\mathbb{S}_{tx_1}$ will be better than that of scheme 2 with signal set $\mathbb{S}_{tx_2}$, if $d^{(1)}_{\min,\mathbf{H}} > d^{(2)}_{\min,\mathbf{H}}$. The ratio of the minimum distances gives the SNR gap between their BER performance at high SNRs, i.e., the SNR gap in dB is

$$\text{SNR}_{\text{gap}} = 20\log\left(d^{(1)}_{\min,\mathbf{H}} / d^{(2)}_{\min,\mathbf{H}} \right). \tag{16}$$

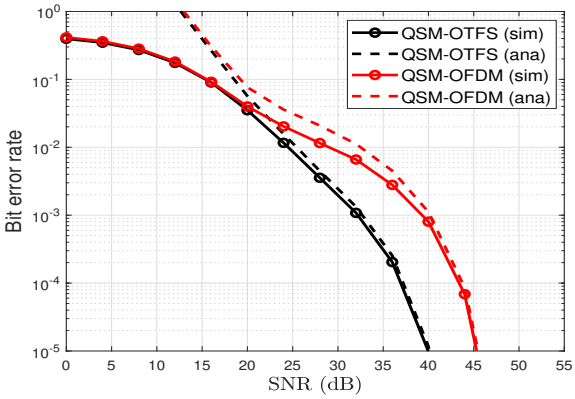

Fig. 5: BER performance of QSM-OTFS ($M = N = 2$, 4-QAM, 2.5 bpcu) and QSM-OFDM ($M = 4$, 4-QAM, 2.5 bpcu) with Rx placed at (3,3).

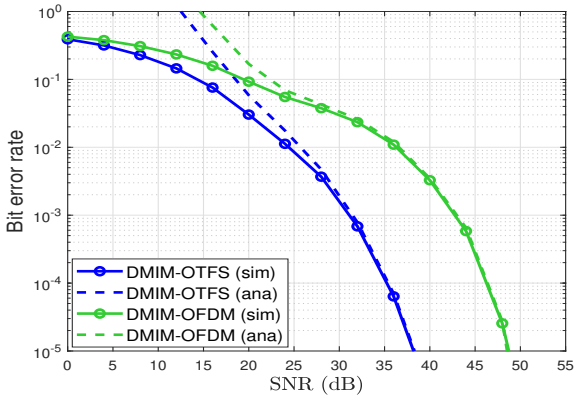

Fig. 6: BER performance of DMIM-OTFS ($M = N = 2$, $\mathbb{S}_A$=4-QAM, $\mathbb{S}_B$=BPSK, 2.25 bpcu) and DMIM-OFDM ($M = 4$, $\mathbb{S}_A$=4-QAM, $\mathbb{S}_B$=BPSK, 2.25 bpcu) with Rx placed at (3,3).

We use the metric in (16) to compute and plot the relative performance of different schemes at different spatial positions of the receiver across the room.

V. Results and Discussions

In this section, we present the analytical and simulation results on the performance of the proposed QSM-OTFS and DMIM-OTFS schemes. We also compare these performances with those of the OFDM counterparts, namely, QSM-OFDM and DMIM-OFDM schemes. The placement of the $N_t = 4$ LEDs and $N_r = 4$ PDs are as described in *Note 1* of Sec. II. In addition, the following LED and PD parameters are used in the simulations: mode number $n = 1$, $\Phi_{\frac{1}{2}} = 60°$, $d_{tx} = 2$m, FOV = 85°, responsivity $r = 0.4$ Amps/Watt, and $d_{rx} = 0.1$m.

A. QSM/DMIM OTFS vs QSM/DMIM OFDM

Figure 5 shows the BER performance of QSM-OTFS scheme with $M = 2$ delay bins, $N = 2$ Doppler bins, 4-QAM, and 2.5 bpcu rate. Both analytical bound on BER and simulated BER are plotted. Similar plots for QSM-OFDM with $M = 4$, 4-QAM, and 2.5 bpcu are also shown for comparison. The receiver coordinates are $(X_R, Y_R) = (3, 3)$. It is observed that, as expected, the BER upper bound is tight at high SNRs. It is also observed that the proposed QSM-OTFS scheme outperforms QSM-OFDM. For example, at 10^{-5} BER, QSM-OTFS performs better by about 5 dB, illustrating the superior performance of OTFS compared to OFDM in VLC environments.

Figure 6 shows a similar BER performance comparison between DMIM-OTFS with $M = N = 2$ and DMIM-OFDM with $M = 4$. In both the schemes, the modulation alphabets $\mathbb{S}_A$ and $\mathbb{S}_B$ used are 4-QAM and BPSK, respectively, and the rate of transmission is 2.25 bpcu. The receiver coordinates are $(X_R, Y_R) = (3, 3)$. Here again, it is observed that the proposed DMIM-OTFS scheme outperforms DMIM-OFDM scheme by about 10 dB at 10^{-5} BER.

B. Spatial distribution of relative performance

The BER performance comparisons in Figs. 5 and 6 are done for a fixed receiver location. Since the channel matrix will change with change in receiver location, the BER performance will also change with receiver location. In Figs. 7 and 8, we analyze the performance of the proposed OTFS schemes and their respective OFDM counterparts at different receiver locations across the room. The assessment is made using normalized minimum distance metric defined in Sec. IV-B. We compute the SNR gap (as per (16)) between the OTFS and OFDM schemes at different receiver locations across the room with a spatial resolution of 2.5cm.

Figure 7 shows the spatial plot of SNR gap (in dB) between the proposed QSM-OTFS scheme and the QSM-OFDM scheme with 2.5 bpcu at various receiver locations across the room. We observe that the SNR gap (in dB) between the considered QSM-OTFS and QSM-OFDM schemes is positive (i.e., QSM-OTFS performs better then QSM-OFDM) in most receiver locations and negative (i.e., QSM-OFDM performs better then QSM-OTFS) in other locations. The fraction of receiver locations where OTFS performs better is captured in the subfigure in Fig. 7, where the locations with positive and negative dB values of SNR gap are marked in yellow and blue, respectively, showing the spatial distribution of the relative performance. It can be seen QSM-OTFS outperforms QSM-OFDM in 78% of the room.

Figure 8 shows a similar spatial performance comparison between the proposed DMIM-OTFS scheme and the DMIM-OFDM scheme, both using symbols from 4-QAM ($\mathbb{S}_A$) and BPSK ($\mathbb{S}_B$) and having 2.25 bpcu rate. As before, in the subfigure, the receiver locations with positive dB SNR gap are marked in yellow and those locations with negative dB SNR gap are marked in blue. It can be observed from the subfigure that the proposed DMIM-OTFS scheme outperforms DMIM-OFDM in 85% of the room area.

C. QSM-OTFS vs DMIM-OTFS

Figure 9 shows the BER performance comparison between QSM-OTFS scheme with $M = N = 2$, 4-QAM, 2 bpcu, and DMIM-OTFS scheme with $M = N = 2$, 4-QAM ($\mathbb{S}_A$), BPSK ($\mathbb{S}_B$), 2.25 bpcu. The receiver location is $(X_R, Y_R) = (2.5, 2.5)$. It can be seen from Fig. 9 that for comparable rate

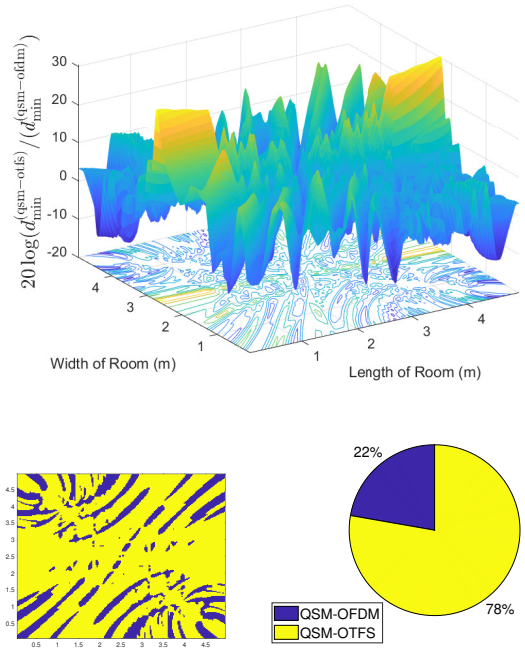

Fig. 7: Spatial distribution of relative normalized $d_{\min}$ of QSM-OTFS and QSM-OFDM with 2.5 bpcu.

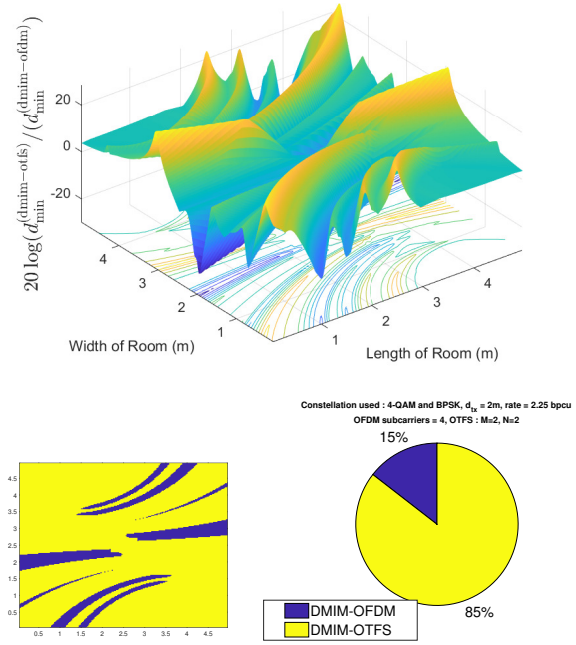

Fig. 8: Spatial distribution of relative normalized $d_{\min}$ of DMIM-OTFSand DMIM-OFDM with 2.25 bpcu.

of transmission, DMIM-OTFS performs better compared to QSM-OTFS (e.g., by about 22 dB at 10^{-5} BER). This is because the average relative distance between transmit signal matrices (i.e., $\mathbf{E}[|\mathbf{X}_1 - \mathbf{X}_2|]$, where $\mathbf{X}_1$ and $\mathbf{X}_2$ are two transmit signal matrices) is higher for DMIM-OTFS due to frame indexing.

VI. Conclusions

We investigated the use of the recently introduced OTFS modulation in indoor multi-LED VLC systems. We proposed two multi-LED schemes, namely, QSM-OTFS and DMIM-OTFS schemes, and evaluated their bit error performance through analysis and simulations. Both the schemes do not require Hermitian symmetry or DC bias operations. Our results showed superior performance of the proposed QSM-OTFS and DMIM-OTFS schemes compared to those of QSM-OFDM and DMIM-OFDM schemes, respectively. The superior performance of OTFS in VLC systems demonstrated in this paper can potentially motivate further research on other possible MIMO VLC architectures using OTFS.

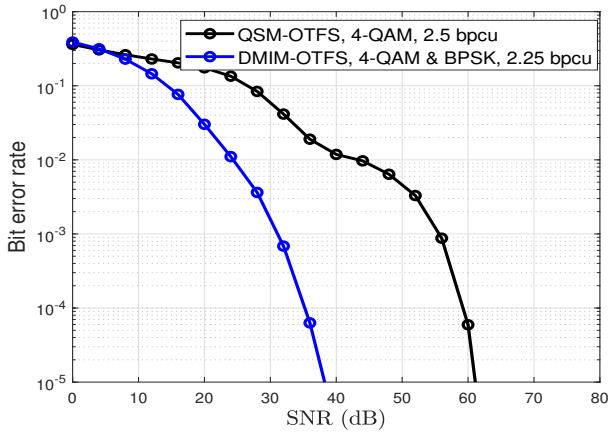

Fig. 9: BER performance of QSM-OTFS ($M = N = 2$, 4-QAM, 2.5 bpcu) and DMIM-OTFS ($M = N = 2$, $\mathbb{S}_A$=4-QAM, $\mathbb{S}_B$=BPSK, 2.25 bpcu) with Rx placed at (2.5,2.5).

References

[1] P. H. Pathak, X. Feng, P. Hu, and P. Mohapatra, "Visible light communication, networking, and sensing: a survey, potential and challenges," *IEEE Commun. Surveys & Tut.*, vol. 17, no. 4, pp. 2047-2077, 2015.

[2] A. Memedi and F. Dressler, "Vehicular visible light communications: a survey," *IEEE Commun. Surveys & Tut.*, vol. 23, no. 1, pp. 161-181, 2021.

[3] Z. Wang, Q. Wang, W. Huang, and Z. Xu, *Visible Light Communications: Modulation and Signal Processing*, Wiley-IEEE Press, 2018.

[4] R. Hadani et al., "Orthogonal time frequency space modulation," *IEEE WCNC'2017*, pp. 1-6, Mar. 2017.

[5] R. Hadani et al., "Orthogonal time frequency space modulation," available online: arXiv:1808.00519v1 [cs.IT] 1 August 2018.

[6] K. R. Murali and A. Chockalingam, "On OTFS modulation for high-Doppler fading channels," *ITA'2018*, Feb. 2018.

[7] P. Raviteja, K. T. Phan, Y. Hong, E. Viterbo, "Interference cancellation and iterative detection for orthogonal time frequency space modulation," *IEEE Trans. Wireless Commun.*, vol. 17, pp. 6501-6515, Oct. 2018.

[8] P. Raviteja, E. Viterbo, Y. Hong, "OTFS performance on static multipath channels," *IEEE Wireless Commun. Lett.*, vol. 8, pp. 745-748, Jun. 2019.

[9] J. Zhong, J. Zhou, W. Liu, and J. Qin, "Orthogonal time-frequency multiplexing with 2D Hermitian symmetry for optical-wireless communications," *IEEE Photon. Jl.*, vol. 12, no. 2, pp. 1-10, Apr. 2020.

[10] R. Mesleh, S. S. Ikki, and H. M. Aggoune, "Quadrature spatial modulation," *IEEE Trans. Veh. Tech.*, vol. 64, no. 6, pp. 2738-2742, Jun. 2015.

[11] T. Mao, Z. Wang, Q. Wang, S. Chen, and L. Hanzo, "Dual-mode index modulation aided OFDM," *IEEE Access*, vol. 5, pp. 50-60, Feb. 2017.

[12] T. L. Narasimhan, R. Tejaswi, and A. Chockalingam, "Quad-LED and dual-LED complex modulation for visible light communication," available online: arXiv:1510.08805v3 [cs.IT] 24 Jul 2016.

[13] K. V. S. S. Sushanth and A. Chockalingam, "Multiple-LED complex modulation schemes for indoor MIMO VLC Systems, *IEEE ICC'2019*, pp. 1-6, May 2019.